Available online at www.sciencedirect.com

SCIENCE DIRECT®

Surface Science 550 (2004) 8–14

SURFACE SCIENCE

www.elsevier.com/locate/susc

Regular step formation on concave-shaped surfaces on 6H–SiC(0 0 0 1)

Wulf Wulfhekel [a,1], Dirk Sander [a,1], Serge Nitsche [a], Frédéric Dulot [a,c], André Leycuras [b], Margrit Hanbücken [a,*]

[a] *CRMC2-CNRS, Campus de Luminy, Case 913, F-13288 Marseille, France*
[b] *CRHEA-CNRS, Rue Bernard Gregory, Sophia-Antipolis, F-06560 Valbonne, France*
[c] *Faculté des Sciences et Technologies, 4, rue des Frères Lumière, F-68093 Mulhouse, France* [2]

Received 26 September 2003; accepted for publication 14 December 2003

Abstract

A concave-shaped surface has been prepared in a 6H–SiC(0 0 0 1) substrate by mechanical grinding. As a consequence, the different crystallographic planes building up the 6H–SiC polytype are cut under continuously changing polar angles in all azimuthal directions. Through hydrogen etching, this curved surface breaks up into a whole set of surfaces vicinal to the initial 6H(0 0 0 1) orientation. The local structural reorganisation after hydrogen etching has been studied by scanning electron microscopy (SEM) and atomic force microscopy (AFM). Two types of local bond environments are present at the step edges leading to a strong anisotropy in the surface etching with hydrogen. As a result, the distribution of the terrace width and the step heights varies with the azimuthal angle and reflects the sixfold symmetry of the bulk crystal. For most azimuthal directions, an alternation of large and small terraces, separated by steps of 0.75 nm heights (height of half the 6H polytype, three bilayers) is observed and only for well defined azimuthal directions, equally spaced terraces separated by steps of 1.5 nm height (one unit cell of 6H–SiC, six bilayers) are found. In addition, the polar variations have been studied by taking various line-scans along the concave-shaped surface with AFM. It seems that for polar angles above 3°, step bunching of several SiC steps occurs whereas below 3° the bimodal terrace width distribution is observed.

Keywords: Silicon carbide; Hydrogen molecule; Etching; Scanning electron microscopy (SEM); Atomic force microscopy; Curved surfaces; Surface structure, morphology, roughness, and topography

1. Introduction

Silicon carbide has become a very important semiconductor material and vicinal silicon carbide surfaces are increasingly used as substrates to grow either thin silicon carbide films or nitrides for device fabrication [1]. A detailed understanding of vicinal silicon carbide surfaces is of great

---

[*] Corresponding author. Fax: +33-491-418-916.
E-mail address: margrit.hanbucken@crmc2.univ-mrs.fr (M. Hanbücken).

[1] On leave of absence from Max-Planck-Institut für Mikrostrukturphysik, Weinberg 2, D-06120 Halle, Germany.

[2] New address.

0039-6028/$ - see front matter © 2004 Elsevier B.V. All rights reserved.
doi:10.1016/j.susc.2003.12.037

importance for both, fundamental SiC growth experiments as well as for technological applications [2]. Undesired screw dislocations observed in GaN films are reduced on vicinal surfaces [3]. The linear alignment of GaN quantum dots on AlN layers grown on vicinal SiC substrates has also been reported [4]. Step structure, step height and terrace width are the parameters which largely determine homo- and heteroepitaxial growth on SiC surfaces. Controlling the step density by introducing certain off-orientations allows the growth of SiC films with one defined crystallographic structure (single polytype) via the so called "step controlled epitaxy" [5]. Silicon carbide films can also be grown with different crystallographic structures, i.e. polytypes, where each polytype is accompanied by specific electronic properties. A large spread in the band-gap energies ranging from e.g. 2.39 eV for the zinc blende 3C–SiC type to 3.33 eV for the wurtzite structured 2H–SiC type has been measured [1]. The polytype growth is influenced by the vicinality (misorientation from a nominal surface orientation, like e.g. (0 0 0 1)) of the SiC substrate. Changing the vicinality locally on the same substrate could allow the controlled growth of different SiC polytypes and implicitly of films with different electronic properties. In previous experiments on silicon, a universal sample for the study of vicinal surfaces has been obtained by transforming concave-shaped surfaces into an extended set of vicinals through thermal treatment [6,7]. In the case of Si(1 1 1) these curved surfaces split up into terraces and steps whose morphology and size distribution reflect the threefold symmetry of the crystal. In extension of our previous work on Si, our objective is to investigate the influence of a locally varying misorientation of a SiC sample on the final morphological and structural changes induced by H_2 etching. In preliminary experiments [8] we have observed first morphological reorganisations of concave-shaped surfaces when they were etched and annealed to 1700 °C. The obtained morphology showed a considerable roughness, while steps were aligned in some preferential directions. Here, we present successful etching conditions leading to regular and smooth structural reorganisations of the initially rough surfaces.

2. Experimental

The samples (4×15 mm^2) were cut from an on-axis, nitrogen doped, n-type (resistivity 0.03–0.12 Ωcm) 6H–SiC(0 0 0 1) wafer [9]. A concave-shaped surface depression was created in the middle of the sample by a dimple grinder (diameter 15 mm), using diamond paste with a grain size of 3 μm. Grinding was stopped when a depth of about 30 μm was obtained in the middle of the dimple. The diameter of the dimple was about 1.5 mm, as checked by scanning electron microscopy (SEM). For the given geometry, the in-plane azimuthal angle φ varied from $0° < \varphi < 360°$ and the out-of-plane polar angle θ from $0° < \theta < 5°$. Some samples were additionally ion milled in a commercial ion mill (Gatan 600) to eliminate the scratches induced by the dimple grinding. Prior to hydrogen (H_2) etching, the samples were sequentially rinsed in trichloroethylene, acetone and methanol in an ultrasonic bath. H_2 etching was performed in a horizontal hot-wall graphite chemical vapour deposition reactor [10] at an H_2 pressure of 13 mbar. The samples were etched at 1800 °C for between 20 min and 1 h. The results were compared to those obtained in previous experiments at an etching temperature of 1700 °C and equal etching intervals [8]. At this high temperature, thermal decomposition of SiC has to be anticipated, leading to the so-called sublimation etch of SiC [11]. In our study, we observe step heights of three SiC bilayers, which indicates that H-etching is the predominant etch mode. The etched samples were subsequently characterised by SEM and atomic force microscopy (AFM) [12]. To follow the influence of the etching process on the various vicinal SiC surfaces, successive line scans were taken through the dimple. For comparison, images were also taken on the flat parts of the SiC substrate outside the dimpled area. Furthermore, no significant structural differences after H-etching were observed on ion-milled substrates, as compared to dimple grinded substrates.

3. Results and discussion

After erosion, all 6H–SiC(0 0 0 1) samples were first characterized on the flat parts in vicinity of the dimpled concave-shaped areas. The initial roughness of the flat parts of the sample was removed through H_2 etching as known from the literature [13]. The observed small corrugation on these parts was, in our experiments, taken as a quality test for the erosion. Successful erosion removed all scratches from the nominal parts of the substrate and gave rise to a well defined distributions of flat terraces and steps. Straight steps of 0.75 or 1.5 nm corresponding to half or the complete lattice distance in the *c*-axis (three or six SiC bilayers) were observed. Within the concave area, the etching rate is reduced as the rate depends on the misorientation of the substrate. The H_2 etch rate of misoriented surfaces can be reduced by 30–40% compared to flat SiC surfaces [14]. Fig. 1 reproduces SEM images taken on two samples after two different treatments. Image (a) was taken on a sample after an erosion at 1700 °C for 1 h [8]. The overall surface morphology is irregular but preferential step-edge orientations can be seen on the image. These stable and straight step edges are oriented along $\langle 1 1 \bar{2} 0 \rangle$ directions. Heating the sample to 1800 °C for 20 min leads to a considerable change in the surface morphology. As seen in the SEM images in Fig. 1(b) and (c), the initial rough irregularities were removed and smooth terraces separated by regular steps were obtained. Although taken on the curved parts of the sample, the relatively low step densities seen in (b) and (c) indicate a polar misorientation close to nominal.

The detailed structural rearrangements with changing polar and azimuthal misorientation were studied using AFM scans across the concave-shaped surface. All observed areas within the curved surface were found to be rearranged in atomically flat terraces separated by straight steps. The step heights in all studied areas was 0.75 or 1.5 nm like on the flat parts of the substrate. The terrace width varied as expected with changing polar angle. Fig. 2 represents five AFM images taken along a line across the curved surface as

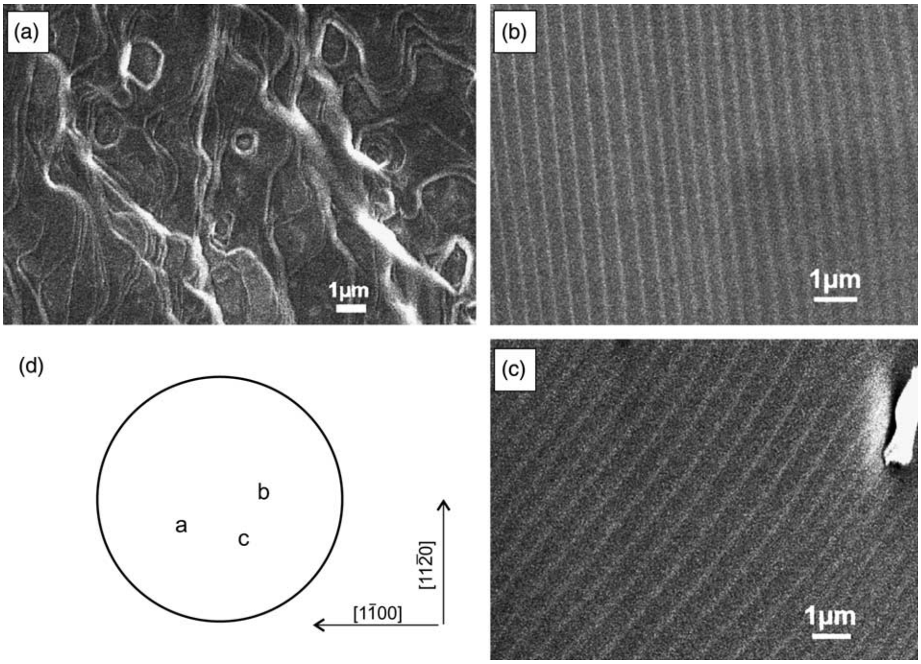

Fig. 1. SEM images obtained at different parts in the concaved-shaped 6H–SiC(0 0 0 1) surface after different heat treatments. A weak step-edge contrast allows the observation of steps and step bunches. Image (a) was taken on a sample after H_2 etching for 1 h at 1700 °C, images (b and c) on a sample after H_2 etching for 20 min at 1800 °C. The areas where images were taken within the concave-shaped surface and the crystallographic directions are given in the sketch (d).

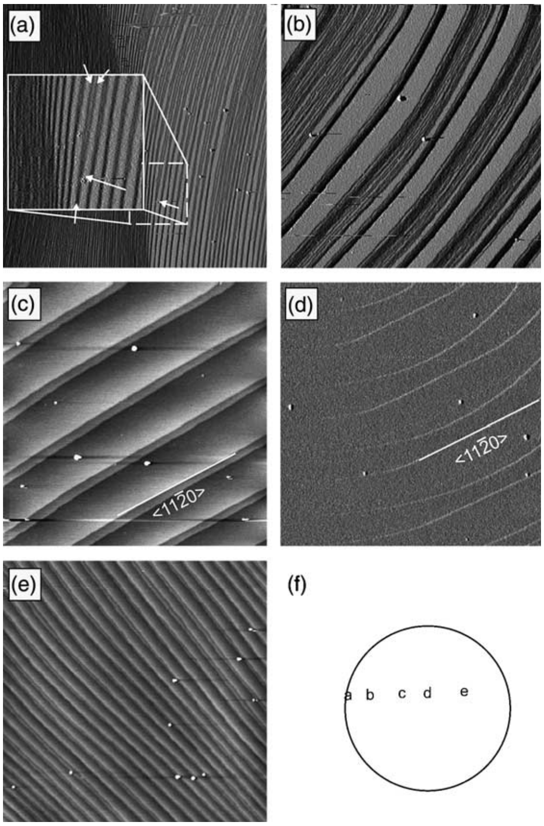

Fig. 2. AFM images obtained along a line across the concave-shaped surface. The sample has been treated by an H_2 erosion at 1800 °C for 20 min. All images are 3 μm × 3 μm in size. The polar misorientation changes from (a) to (e). The approximate values of the polar misfit are: (a) nominal misfit of flat surface, (b) polar misfit 5°, (c) polar misfit 2°, (d) polar misfit 0°, (e) 3°. The positions of the scans within the concave-shaped surface depression are indicated in the sketch (f). The white lines indicate the $\langle 1\,1\,\bar{2}\,0\rangle$ direction of straight steps. The inset of Fig. 2(a) is a magnified view to indicate the splitting of a six-bilayer high step into two three-bilayer high step.

indicated in the sketch. Fig. 2(a) focuses on the rim of the depression. On the left, 1.5 nm high steps are observed with an average step distance of about 25 nm which is due to the miscut of the nominally flat surface of the wafer. Entering the concave-shaped surface, first the step density decreases. This effect is due to a compensation of the misorientation. Interestingly, one observes that most of the six bilayer high steps split up in pairs of three bilayer high steps, as indicated by the arrow, and by the inset of Fig. 2(a). This indicates that at lower miscut, i.e. lower step density, six-bilayer high steps may become unstable and split up into two three-bilayer high steps. This effect can be driven by a repulsive step–step interaction or simply by an higher entropy of the split step. Moving over the edge further into the concave-shaped surface, the polar misorientation and consequently the step density increases as can be seen in Fig. 2(b). At this high a density, regular steps are no more favourable but step bunching is observed. This indicates an instability of the highly miscut surface. Step bunching was only observed in the outer part of the dimpled depression with nominal misorientation of about 3–5°. Further towards the centre of the depression, regular and straight steps are observed cf. Fig. 2(c)–(e). In the areas of low step densities, six and three bilayer high steps are found. In case of three bilayer high steps (see Fig. 2(c) and (e)), a bimodal terrace width distribution occurs [8], which will be discussed in more detail below. Near the centre of the concave-shaped surface (see Fig. 2(d)), the step density is extremely low and exclusively 0.75 nm steps are found. Interestingly, these steps show curved and straight segments, which are not due to step–step interaction as there is no obvious correlation between the shape of a step and the position of the neighbouring steps. It is proposed that the step curvature is related to the azimuthal angle of the step edge, and therefore to the crystallography of the sample surface.

In the following, we concentrate on the bimodal terrace width distribution and relate this to the azimuthal dependence of the step shape. This azimuthal dependence is related to the complex layer structure of 6H–SiC. Along the *c*-axis of the crystal, the SiC double layers of threefold symmetry are arranged in two groups of three double layers each. Within each group, the stacking is hcp, but from one group to the other, the lattice is rotated by 60°. As a consequence, the close packed step edges on 6H–SiC change their nature going from one group to the other. The character of steps running along low index directions alternates and shows either one (SN) or two (SD) dangling bonds per carbon atom (step nomenclature according to Pechman et al. [15]). The exclusive observation of step heights of a multiple of 0.75

nm indicates that there is a strong attractive interaction between the bilayer steps within one group. They always cluster and form a three bilayer high step as indicated in Fig. 3(a). At large miscuts, the two three bilayer high steps pair up to form six bilayer high steps of 1.5 nm height with a micro-facet at the step edge. For this, a short range attractive step–step interaction is needed, that overcomes the entropic step repulsion [16] of the pairs of three bilayer steps. This attractive step–step interaction has the potential to induce also the observed step bunching at miscuts above 3°, see Fig. 2(b).

On top of this, the crystal structure of 6H–SiC(0 0 0 1) adds to the complexity of the surface morphology at lower step concentrations, where the six bilayer steps split up into three bilayer steps. The different atomic structures at the SN and SD step edges may lead to different etch rates during H_2 exposure. Let us assume—without loss of generality—that the SD step edges with their two dangling bonds are more reactive leading to a higher etch rate and by this a higher speed of recession during etching. Along closed packed directions, this should lead to the situation that the SD steps run into SN steps. As a consequence, a

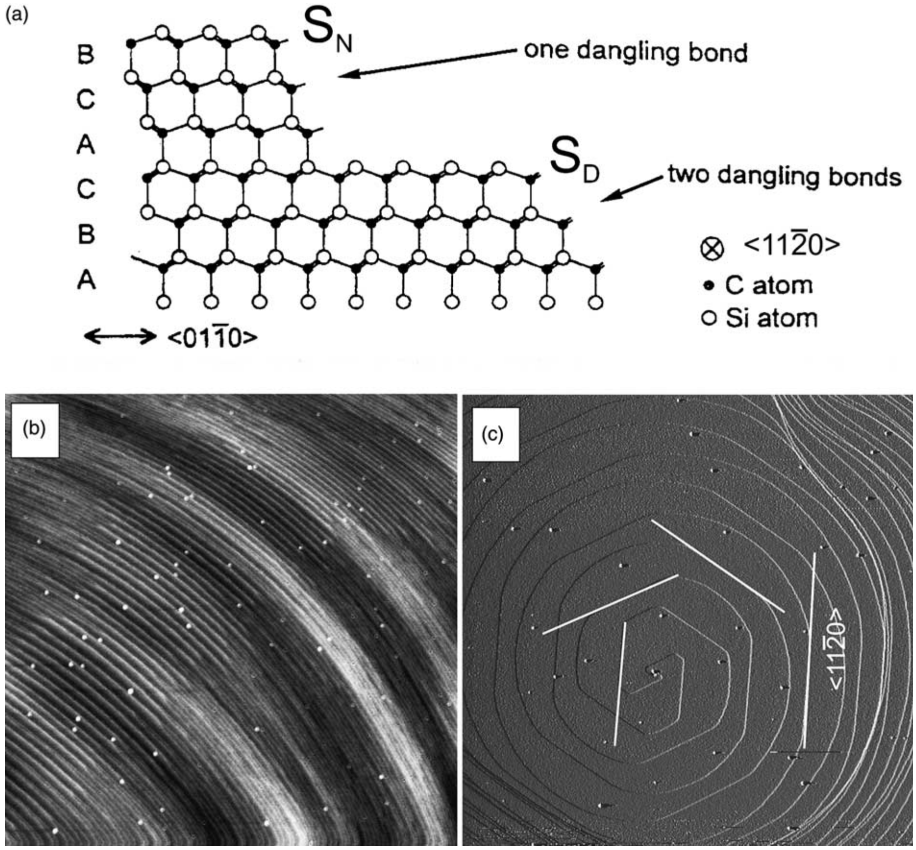

Fig. 3. Schematics of the atomic structure and the dangling bonds at step edges (a). AFM images of etched surfaces near the centre of the concave-shaped depression (b and c). (b) Bunching of the two groups of bilayers is observed (see text for details); 3 μm × 3 μm. (c) Morphological variations due to changing azimutal directions around a screw dislocation are shown; 6 μm × 6 μm. The white lines indicate the ⟨1 1 $\bar{2}$ 0⟩ direction of straight steps.

tendency for 1.5 nm high steps should be observed along the closed packed directions. This tendency is experimentally observed as depicted in Fig. 3(b) and (c). At rather low step densities and terrace widths of about 65 nm as in Fig. 3(b), six bilayer steps are formed along closed packed directions due to the mechanism described above. The six bilayer high steps were observed in a small azimuthal segment of the curved surface. When, however, the step direction deviates significantly from closed packed directions, a gradual change of the number of dangling bonds occurs within the two coupled 0.75 nm high steps. Therefore the etching rates of the two 0.75 nm high steps approach each other leading to the separation of the two groups of three layers. Isolated three bilayer high steps are resolved on both azimuthal sides of the region of closed packed steps. Since the steps of the two groups are heavily kinked and contain the same amount of single and double dangling bonds per unit length at 30° azimuthal angles from closed packed directions, they are etched at the same speed and no pairing of the steps is seen at these angles. These characteristic azimuthal variations within the SiC plane around (0 0 0 1) can nicely be studied while looking at closed step loops (mounts or holes) or even better at the surroundings of a screw dislocations. Fig. 3(c) gives an AFM image of a screw dislocation on 6H–SiC where its core creates a small depression. Going once around the core, two steps of 0.75 nm are crossed, i.e., the dislocation shifts the crystal structure by six bilayers keeping the crystallography of the two groups of steps. The low energy steps, i.e. those with one single dangling bond, are favoured by the Wulff construction and appear as straight steps. Within one of the 0.75 nm high steps, three straight segments are found within the full azimuthal range reflecting the threefold symmetry of the bilayers. The straight steps have the larger terraces located above the step-edge indicating their lower etch rate when compared to the rounded step edges of high energy containing two dangling bonds. These show smaller upper terraces indicating a fast etching. As a consequence of the crystallographic structure, alternating pairs of steps of both types approach each other with always the straight, i.e. slow etched, step on the top. When they can come close enough, they can pair up and form 1.5 nm high steps. In this discussion, we assumed that the slowly etched step is the species with only one dangling bond. This agrees with its straight appearance and the Wulff construction. In principle, it could also be the step with two dangling bonds, that is etched slower. This is unlikely, as the two dangling bonds should promote a higher reactivity. In addition, these step edges should be of higher energy compared to the step edges with only one dangling bond, i.e. they should be the shorter and more curved steps in Fig. 3(c). This is in contrast to the experimental finding. Therefore, we conclude that the scenario we used in the paragraphs above, is the more likely one.

Our model neglects the impact of possible structural relaxation or surface reconstruction near the step edges. Such surface reconstructions are efficient ways to reduce the number of dangling bonds, and they are well known for semiconductor surfaces. They also might lead to different etch rates for restructured step regions. However, as we have no experimental evidence for such a restructuring, we propose the simple model above.

The understanding of this complex etching behaviour of 6H–SiC(0 0 0 1) may be used to tailor the morphology of SiC substrates used for epitaxy. Equally spaced 0.75 or 1.5 nm steps may be selected for low miscuts by choosing the azimuthal miscut direction. Step bunching can be induced by miscuts above 3°. Even the number of dangling bonds at the step edges may be influenced.

4. Summary

The H_2 etching conditions allows the transformation of a concave-shaped, dimpled surface of 6H–SiC into an extended set of vicinal surfaces. At miscuts above 3°, step bunching was observed and related to an attractive short range step–step interaction. At miscuts below 3°, regular steps evolve that can either be of 1.5 or 0.75 nm height. The step heights can be controlled for low miscuts by choosing the azimuthal direction of the miscut. This behaviour was traced back to the number of dangling bonds at the step edges and related to that, their etching rate.

Acknowledgements

D.S. and W.W. gratefully acknowledge the friendly hospitality and support by the CRMC2 and the Université d'Aix-Marseille 2. M.H. gratefully acknowledges the friendly hospitality of the Max-Planck-Institut für Mikrostrukturphysik. F.D. gratefully achnowledges the continuous hospitality of the CRMC2.

References

[1] W.J. Choyke, in: R. Freer (Ed.), The Physics and Chemistry of Carbides, Nitrides and Borides, (NATO ASI Series, Manchester, 1989).

[2] K. Heinz, U. Starke, J. Bernhardt, J. Schardt, Appl. Surf. Sci. 162–163 (2000) 9.

[3] M.H. Xie, L.X. Zheng, S.H. Cheung, Y.F. Ng, H. Wu, S.Y. Tongand, N. Ohtani, Appl. Phys. Lett. 77 (2000) 1105.

[4] J. Brault, S. Tanaka, E. Sarigiannidou, J.L. Rouviere, B. Daudin, G. Feuillet, H. Nakagawa, J. Appl. Phys. 93 (2003) 3108.

[5] T. Ueda, H. Nishino, H. Matsunami, J. Crystal Growth 104 (1990) 695.

[6] M. Hanbücken, B. Röttger, R. Kliese, I. Vianey, H. Neddermeyer, Europhys. Lett. 23 (1993) 573.

[7] M. Hanbücken, B. Röttger, H. Neddermeyer, Surf. Sci. 331–333 (1995) 1028.

[8] F. Dulot, L. Mansour, A. Leycuras, W. Wulfhekel, D. Sander, F. Arnaud d'Avitaya, M. Hanbücken, Appl. Surf. Sci. 187 (2002) 319.

[9] A.G. SiCrystal, Erlangen, Germany, www.sicrystal.de.

[10] A. Leycuras, Mater. Sci. Forum 338–342 (2000) 241.

[11] F. Owman, C. Hallin, P. Mårtensson, E. Janzén, J. Cryst. Growth 167 (1996) 391.

[12] Nanoscope, Digital Instruments.

[13] N. Ohtani, M. Katsuno, T. Aigo, T. Fujimoto, H. Tsuge, H. Yashiro, M. Kanaya, J. Crystal Growth 210 (2000) 613; C. Hallin, F. Owman, P. Martensson, A. Ellison, A. Konstantinov, O. Kordina, E. Janzen, J. Crystal Growth 181 (1997) 241.

[14] Z.Y. Xie, C.H. Wei, L.Y. Li, Q.M. Yu, J.H. Edgar, J. Crystal Growth 217 (2000) 115.

[15] R.J. Pechman, X.-S. Wang, J.H. Weaver, Phys. Rev. B 52 (1995) 11412.

[16] C. Jayaprakash, C. Rottmann, W.F. Saan, Phys. Rev. B 30 (1984) 6549.